ANALYTICAL BIOCHEMISTRY 211, 7-15 (1993)

A Continuous Spectrophotometric and Fluorimetric Assay for Protein Tyrosine Phosphatase Using Phosphotyrosine-Containing Peptides

Zhong-Yin Zhang,* Derek Maclean,† Andrea M. Thieme-Sefler,† Roger W. Roeske,‡ and Jack E. Dixon*,[1]

*Department of Biological Chemistry, Medical School, The University of Michigan, Ann Arbor, Michigan 48109, and the Walther Cancer Institute; †Parke-Davis Research Division, Warner Lambert Company, Ann Arbor, Michigan 48105; and ‡Department of Biochemistry and Molecular Biology, Indiana University School of Medicine, Indianapolis, Indiana 46202

Received November 9, 1992

Two continuous assays for protein tyrosine phosphatases (PTPases) have been developed using phosphotyrosine containing peptide substrates. These assays are based on the marked differences in the spectra of the peptide before and after the removal of the phosphate group. The increase in the absorbance at 282 nm or the fluorescence at 305 nm of the peptide upon the action of PTPase can be followed continuously and the resulting progress curve (time course) can be analyzed directly using the integrated form of the Michaelis–Menten equation. The procedure is convenient and efficient, since both k_{cat} and K_m values can be obtained in a single run. The difference absorption coefficient ($\Delta\epsilon$) at 282 nm is relatively insensitive to the pH of the reaction media. These techniques were applied to two homogeneous recombinant PTPases employing six phosphotyrosine-containing peptides. K_m and k_{cat} values obtained from the progress curve analysis were similar to those determined by the traditional initial rate inorganic phosphate assay. The peptides corresponding to autophosphorylation sites in Neu, p56^{lck}, and p60^{src} proteins show distinct behavior with the *Yersinia* PTPase, Yop51*, and the mammalian PTPase (PTP1U323). In both cases, the k_{cat} values were relatively constant for all the peptides tested whereas the K_m values were very sensitive to the amino acid sequence surrounding the tyrosine residue, especially in the case of Yop51*. Thus, both Yop51* and PTP1U323 show differential recognition of the phosphotyrosyl residues in the context of distinct primary structure of peptide substrates.

Protein tyrosine phosphorylation in the cell plays a major role in the regulation of signal transduction (1). Protein tyrosine phosphatases (PTPases),[2] which exclusively remove phosphate from tyrosine residue in proteins, are crucial components in controlling the overall level of tyrosine phosphorylation (2). Detailed knowledge of the specific functions of PTPases requires a thorough understanding of their substrate specificities. There are a limited number of studies on the substrate specificity of the PTPases and many of these utilize a variety of "artificial" substrates such as tyrosine-phosphorylated casein, RCM-lysozyme, myelin basic protein, and reduced, carboxamidomethylated bovine serum albumin (3,4). Synthetic peptides such as tyrosine phosphorylated Raytide, angiotensin, and the src-peptide have also been employed as "model" substrates (5,6). In these assay systems, the protein or peptide is usually phosphorylated using an appropriate kinase and [γ-^{32}P]ATP. The PTPase activity is determined by measuring the release of [^{32}P]phosphate from the phosphoprotein or phosphopeptide. The low stoichiometry of the kinase reaction, the possibility of multiple and nonspecific phosphate incorporation, and the limited amount of phosphorylated substrate that can be prepared are all limitations of this approach. Recent progress in solid-phase peptide synthesis has resulted in the successful preparation of tyrosine-phosphorylated peptides (7,8). This has made possible the preparation

[1] To whom correspondence should be addressed. Fax: (313)763-4581.

[2] Abbreviations used: PTPases, protein tyrosine phosphatases; pNPP, *p*-nitrophenyl phosphate; DMAP, 4-dimethylaminopyridine; HOBt, *1-hydroxybenzotriazole*; DCC, *N,N'*-dicyclohexylcarbodiimide; DMF, dimethylformamide; DCM, dichloromethane; NMP, *N*-methylpyrrolidone; THF, tetrahydrofuran; EDT, 1,2-ethanedithiol; TFA, trifluoroacetic acid.

0003-2697/93 $5.00

of larger quantities of peptides which are stoichiometrically phosphorylated on specified tyrosine residues. This sets the stage for careful kinetic and mechanistic studies, as well as substrate specificity investigation on PTPases.

There are generally two types of assay for the synthetic phosphopeptide substrates. One is to follow the PTPase-catalyzed hydrolysis by measuring the production of inorganic phosphate using the malachite green colorimetric assay (9), and the other is to follow the breakdown of peptide substrates by HPLC, since the phosphorylated and dephosphorylated forms have different retention times (10). These two techniques are discontinuous assays and the procedures are laborious. Initial rates are generally measured and large quantities of substrate are needed. For substrates with low K_m values (μM range), the inorganic phosphate colorimetric assay is inappropriate due to the inherently low sensitivity.

Efforts to monitor phosphatase catalysis by a continuous spectrophotometric assay have employed low-molecular-weight phosphate monoesters such as *p*-nitrophenyl phosphate (pNPP), β-naphthyl phosphate, and tyrosine phosphate. Two recent papers describe the spectrophotometric assays for acid and alkaline phosphatase (11) as well as PTPases (12) using tyrosine phosphate as a substrate. Since tyrosine phosphate structurally resembles the most commonly used "artificial" PTPase substrate pNPP, one would not anticipate that it will yield fundamentally different kinetic properties from that of pNPP.

In this paper, we describe a continuous spectrophotometric and fluorimetric assay for protein tyrosine phosphatase using synthetic, tyrosine-phosphorylated peptide substrates. These methods exploit the fact that there is a significant spectrophotometric and fluorimetric change in the spectra of the peptide substrate before and after removal of the phosphate group from a tyrosine residue. In addition, we have applied the integrated Michaelis–Menten equation to the analysis of the progress curves of PTPases catalyzed dephosphorylation of the synthetic peptide substrate, so that both Michaelis–Menten kinetic parameters (k_{cat} and K_m) could be obtained in a single experiment. We report the application of this technique to two purified PTPases from bacteria and mammals. The technique has a number of advantages including the small amount of substrate needed for K_m and k_{cat} determinations as well as being both rapid and continuous.

MATERIALS AND METHODS

Materials

All amino acids are of L configuration. Purchased reagents were obtained from the following sources: Nα-Fmoc Tyr, Bachem Bioscience; all other Nα-Fmoc and NαBoc–amino acids, Applied Biosystems (ABI) or Bachem California; *p*-alkoxybenzyl alcohol polystyrene resin, ABI; piperidine, 4-dimethylaminopyridine (DMAP), 1-hydroxybenzotriazole (HOBt), *N,N'*-dicyclohexylcarbodiimide (DCC), ABI; methanol (MeOH), *N,N*-dimethylformamide (DMF), dichloromethane (DCM), *N*-methylpyrrolidone (NMP), Burdick and Jackson (high purity grade); tetrahydrofuran (THF), 1*H*-tetrazole, 1,2-ethanedithiol (EDT), anisole, di-t-butyl-*N,N*-diethylphosphoramidite, thioanisole, and 70% aqueous *t*-butyl hydroperoxide, Aldrich Chemical; trifluoracetic acid (TFA), Halocarbon Products; H_2O and CH_3CN (HPLC quality), EM Science.

Enzyme Preparation

Homogeneous recombinant *Yersinia* PTPase, Yop51* (13), and the mammalian PTPase, PTP1U323 (14), were purified as described. Enzyme and peptide substrate concentrations were determined by amino acid analysis.

Peptide Substrate Preparation

Peptide synthesis. The peptides were prepared by standard solid phase peptide methodology (on a 0.25-mmol scale) (15) on an ABI 431A Peptide Synthesizer using the Fmoc/OtBu (ABI Standard Fmoc Version 1.12) strategy. Single couplings were carried out with four equivalents of the protected amino acid activated ester formed by reaction with DCC and HOBt. A typical cycle for the coupling of an individual amino acid was: (i) deprotection with 20% piperidine in NMP, 21 min; (ii) washes with NMP, 9 min; (iii) coupling of the HOBt activated ester in NMP, 71 min; and (iv) washes with NMP, 7 min. Coupling of the first amino acid to the resin was carried out in the presence of DMAP (0.1 equivalents). After completion of the synthesis, the protected peptide resin was washed with DCM and dried at reduced pressure. All amino acids used were the standard Fmoc derivatives available from ABI with two exceptions. First, when required, the tyrosine was incorporated with the phenolic hydroxy group unblocked, so as to render it available for phosphorylation. Second, whenever the amino acid was available, the N-terminal amino acid was incorporated as its Nα-tertiary-butoxycarbonyl (t-Boc) derivative such that cleavage of this N-terminal protecting group could be achieved concomitantly with cleavage of the peptide from the resin rather than require a separate cleavage step.

Peptide phosphorylation (16). A portion of the protected peptide resin was washed with DMF, DCM, and dry THF (distilled over sodium/benzophenone). To the resin was added 20 ml of dry THF, followed by 50 equiva-

lents of di-t-butyl-*N,N*-diethylphosphoramidite, and then 150 equivalents of 1*H*-tetrazole. The suspension was shaken for 60 min, drained, and washed well with dry THF and DCM. The resin was suspended in 20 ml of DCM and treated with 20 equivalents of a 70% aqueous solution of *t*-butyl hydroperoxide and shaken for 60 min. The suspension was drained, and the resin was washed with DCM, DMF, and DCM and dried under reduced pressure.

Peptide cleavage and purification. The peptide was removed from the resin by treatment with 95% aqueous TFA (10 ml) for 2 h. EDT, anisole, and/or thioanisole (0.5 ml each) were added as required (15). After concentration in vacuum, filtration with ET_2O gave crude peptide. The crude peptide was dissolved in approximately 2 ml of 0.1% TFA (with increasing amounts of TFA as needed for dissolution) and chromatographed on a Vydac 218TP1022 preparative HPLC column (10 μm particle size, 300-Å pore size, 2.2 × 23 cm). A selected gradient of 0.1% TFA in CH_3CN was used to elute the peptide from the column, which was originally in 0.1% TFA. A flow rate of 15 ml/min was maintained on a Waters 600E System Controller and the absorbance of the eluant at 214 nm was recorded on a Waters 490E Programmable Multiwavelength Detector. Individual fractions were collected and analyzed by analytical HPLC on a Vydac 218TP54 analytical HPLC column. Appropriate fractions were combined and concentrated under reduced pressure, diluted with H_2O, and lyophilized to give the product.

Peptide analysis. The peptides were assayed for purity by reversed-phase HPLC on a Vydac 218TP54 analytical column. Comparison of chromatographic traces of crude tyrosine-phosphorylated peptides with those for the corresponding unphosphorylated peptides indicated that peptide phosphorylation had proceeded efficiently, giving 95–100% of the desired product. Following purification as described above, no unphosphorylated contaminant was detected in the pure phosphorylated peptide. All peptides were >98% pure as determined in this manner. In addition, peptide content was determined using combustion microanalysis, and was typically found to be 70–80%, the remainder believed to be residual water and salts. Fast-atom bombardment or electrospray mass spectrometry gave the expected molecular ion, and amino acid analysis was within 10% of the expected values in all cases. ^1H and ^{31}P NMR gave spectra which were in good agreement with predicted values.

Peptide $p60^{src}_{523-531}$ (TEPQpYQPGE) was prepared according to the procedure described by Tian *et al.* (17). RR-src peptide (RRLIEDAEpYAARG) which was based on the sequence surrounding the site of the autophosphorylation in $p60^{src}$ (18) was obtained from the Protein Core facility of the University of Michigan.

Spectroscopy

Spectrophotometric and fluorometric determinations were performed on a Perkin–Elmer lambda 6 UV/vis spectrophotometer and a Perkin–Elmer LS50 fluorometer, respectively. Both instruments were equipped with a water-jacketed cell holder, permitting maintenance of the reaction mixture at the desired temperature.

Buffers

Buffers were prepared as follow: pH 4–5.7, 100 mM acetate; pH 5.8–6.3, 50 mM succinate; pH 6.5–7.3, 50 mM 3,3-dimethylglutarate; and pH 7.5–9.0, 50 mM Tris. All of the buffer systems contained 1 mM EDTA and the ionic strength of the solution was kept at 0.15 M using NaCl. Solutions were prepared using deionized and distilled water. All chemicals were of the highest purity available and were used without further purification.

Continuous Enzyme Assay

All enzyme assays, both spectrophotometric and fluorometric, were conducted at 30°C. For standard spectrophotometric assay, a micro cuvette was used. The pH and ionic strength buffered solution (the total reaction mixture was 500 μl) containing an appropriate amount of peptide substrate was incubated at 30°C for at least 15 min before the reaction was started by introducing a catalytic amount of PTPase into the reaction mixture. The PTPase-catalyzed hydrolysis reaction was followed continuously at 282 nm to completion and the entire time course was stored for data analysis. Identical assay conditions were followed for the fluorometric measurements, except that the reaction volume was 1 ml in a 0.4 × 1.0-cm cuvette. The PTPase-catalyzed hydrolysis reaction was monitored continuously at 305 nm for the increase in tyrosine fluorescence with excitation at 280 nm.

Inorganic Phosphate Assay

To follow the PTPase-catalyzed dephosphorylation of phosphotyrosine-containing peptides by determining the inorganic phosphate produced, a modified inorganic phosphate assay procedure (19) was used. A reaction mixture of 99 μl containing substrate concentration in the range of 0.2 to 5 K_m, 50 mM 3,3-dimethylglutarate, 1 mM EDTA, I = 0.15 M, pH 6.6 buffer, was incubated at 30°C for 15 min. The reaction was initiated by the introduction of 1 μl of PTPase equilibrated in the same buffer. The reaction was quenched by addition of 50 μl of 10% trichloroacetic acid followed by addition of 100 μl of a mixture (composed of 40 μl 2% ammonium molybdate and 60 μl of 14% ascorbic acid in 50% trichloroacetic acid), and then 250 μl of 2% trisodium citrate plus 2% sodium arsenite in 2% acetic acid was added. The color

was developed for 30 min before the absorption at 700 nm was measured.

Data Analysis

The Michaelis–Menten equation is a differential velocity equation and can be written as

$$v = dp/dt = -ds/dt = V/[1 + K_m/s] = V/[1 + K_m/(s_0 - p)], \quad [1]$$

where V is the maximum velocity, K_m is the Michaelis constant, s_0 is the initial substrate concentration, and s and p are the substrate concentration and product concentration at time t. Equation [1] can be rearranged and integrated (20) into Eq. [2]:

$$Vt = \int_0^p [1 + K_m/(s_0 - p)]dp + \text{constant}. \quad [2]$$

When $t = 0$, then $p = 0$. Equation [2] becomes

$$Vt = p + K_m \ln[p_\infty/(p_\infty - p)]. \quad [3]$$

One can transform Eq. [3] to yield an explicit solution for time, t, as a function of the product concentration, p:

$$t = p/k_{cat}E_0 + (K_m/k_{cat}E_0) \ln[p_\infty/(p_\infty - p)]. \quad [4]$$

This relationship can then be used directly to analyze an array of experimental t–s data pairs by nonlinear least squares methods where the parameters k_{cat} and K_m are optimized not through minimizing $\Sigma (p_{exp} - p_{calc})^2$ but $\Sigma (t_{exp} - t_{calc})^2$. In both Eqs. [3] and [4], the product concentration at infinity, p_∞, is equal to the initial substrate concentration, s_0.

The integrated equation derived above is valid over the entire course of the reaction under conditions that there is no product inhibition. For systems which exhibit severe product inhibition, appropriate integrated equations have been derived (21,22, and also see Discussion). The complete time course of the PTPase-catalyzed hydrolysis of tyrosine phosphorylated peptide substrate can be recorded by monitoring the increase in absorbance at 282 nm (or increase in fluorescence at 305 nm with excitation at 280 nm), and the Michaelis–Menten kinetic parameters k_{cat} and K_m can be determined by analyzing the experimental data through a nonlinear least-squares fit algorithm (23) using the integrated Michaelis–Menten equation (Eq. [4]).

RESULTS

Absorbance and Fluorescence Spectra of the Phosphorylated and Dephosphorylated Peptides

Figure 1A shows the ultraviolet absorbance spectra of 397 μM $p60^{src}_{523-531}$ (TEPQpYQPGE) at pH 6.6, before (dashed line) and after (solid line) the phosphate group was removed from the tyrosine residue. Figure 1B shows the fluorescence emission spectra of 15 μM $Neu_{347-357}$ (DAEEpYLVPQQG) at pH 6.6 before (dashed line) and after (solid line) the phosphate group was removed from the tyrosine residue. Similar spectroscopic properties were observed for other peptides examined. It is clear that the attachment of a phosphate group to the tyrosine residue in a polypeptide alters the spectroscopic characteristics of the peptide in such a way that results in a blue shift and reduction in intensity of both tyrosine absorbance and fluorescence spectra. We also found that the change in tyrosine absorbance due to phosphorylation is relatively insensitive to the amino acid sequence surrounding the tyrosine residue. Thus, the different peptides of Table 2 have very similar $\Delta\epsilon$ values at 282 nm. It is not a prerequisite to know the $\Delta\epsilon$ value of each peptide for the determination of kinetic parameters (see Discussion). These observations form the basis for the continuous assay technique for PTPase described below. It is interesting to note that the dephosphorylated and phosphorylated tyrosine containing peptides have similar spectroscopic characteristics to those found for free tyrosine and phosphotyrosine respectively (11,12). As was found for tyrosine and phosphotyrosine (11), the difference in absorbance coefficient at 282 nm ($\Delta\epsilon$) for the dephosphorylated and phosphorylated tyrosine containing peptide is relatively insensitive to the pH of the reaction medium (Table 1).

Progress Curve Analysis

A typical time course of the Yop51*-catalyzed hydrolysis of $p60^{src}$ at pH 6.6, 30°C, followed by the increase in absorbance at 282 nm is shown in Fig. 2A. Figure 2B showed a typical time course of the PTP1U323 catalyzed hydrolysis of $Neu_{347-357}$ at pH 6.6 and 30°C followed by the increase in tyrosine fluorescence at 305 nm with excitation at 280 nm. Data from the progress curves were collected and fitted to the integrated form of the Michaelis–Menten rate equation (Eq. 4). In most cases, two or more different substrate concentrations which were greater than 2 times the K_m value were used for each peptide to check the validity of the analysis. Both k_{cat} and K_m values can be obtained simultaneously from a single run. Table 2 and Table 3 summarize the Michaelis–Menten kinetic parameters of seven phosphotyrosine-containing peptides for Yop51* and PTP1U323 respectively. It is interesting to note that although the k_{cat} values for the Yop51*-catalyzed hydrolyses of the seven peptides were relatively constant (with the exception of $Neu_{546-556}$), the K_m values were extremely sensitive to the amino acid sequence surrounding the phosphotyrosine residue. Thus Yop51* displays a differential recognition of phosphotyrosyl res-

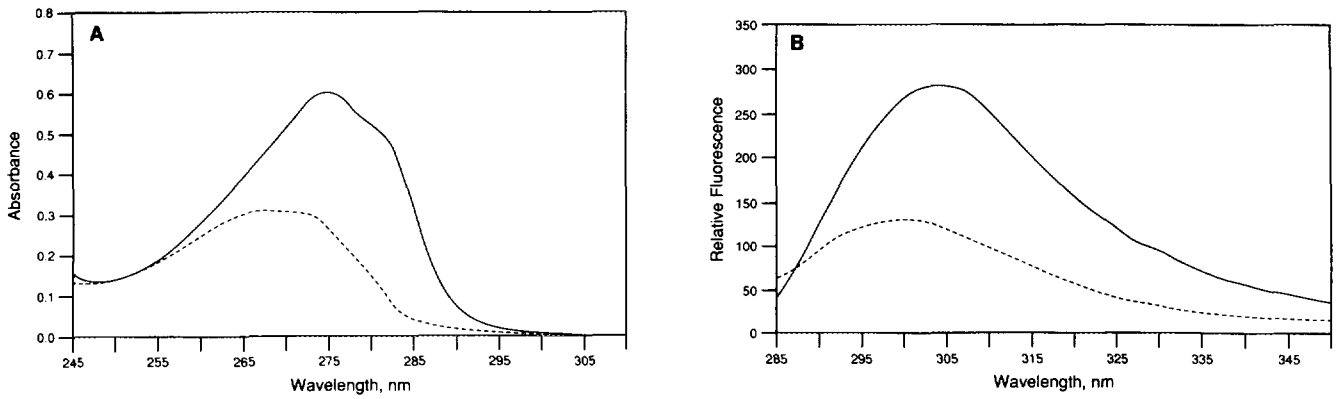

FIG. 1. Ultraviolet absorption spectra and fluorescence emission spectra of phosphotyrosine containing peptides before and after the removal of the phosphate group. (A) Absorption spectra. Spectra were taken at 25°C, in 50 mM 3,3-dimethylglutarate, 1 mM EDTA, I = 0.15 M, pH 6.6 buffer. The peptide $p60^{src}$ concentration was 397 μM. Solid line, dephosphorylated peptide $p60^{src}$; dashed line, tyrosine phosphorylated peptide $p60^{src}$. (B) Fluorescence emission spectra. Fluorescence emission spectra were recorded from 285 to 350 nm (slit width 5 nm) at 25°C in 50 mM 3,3-dimethylglutarate, 1 mM EDTA, I = 0.15 M buffer, with excitation at 280 nm (slit width 3.5 nm). The peptide $Neu_{347-357}$ concentration was 15 μM. Solid line, dephosphorylated peptide; dashed line, tyrosine phosphorylated peptide.

idues in distinct primary structure contexts. This was exemplified by the finding of a more than 20-fold difference in the k_{cat}/K_m ratio (the so-called specificity constant) for Yop51* against these peptides. On the other hand, PTP1U323 not only showed relatively constant k_{cat} values against all the peptides examined, but also only moderate selectivity to the amino acid sequence surrounding the tyrosine residue. This was demonstrated by it showing only a fourfold difference in k_{cat}/K_m ratio among the substrates studied. It is also worthwhile to point out that both Yop51* and PTP1U323 are extremely efficient catalysts, because even at pH 6.6, 30°C, the k_{cat}/K_m values approach the diffusion controlled limit. For peptides that contain Trp residue(s), the progress curve analysis assay is still applicable when the K_m of the peptide is low, i.e., low substrate concentration can be used and the background due to the absorbance of Trp can be blanked out. Figure 3 displays the uv absorption spectra of 104 μM $Neu_{546-556}$ before and after the removal of the phosphate from the tyrosine residue at pH 6.6. The difference spectrum is shown in Figure 3 inset, the maximum difference in absorption being at 283 nm ($\Delta\epsilon$ = 984). In fact, the k_{cat} and K_m values for the PTP1U323-catalyzed hydrolysis of peptide $Neu_{546-556}$ (DNLYpYWDQNSS) (see Table 3) were obtained using the same continuous assay procedure. However, if the K_m of the Trp-containing peptide is high, for example greater than 100 μM, initial rate assay using either HPLC or inorganic phosphate determination remains the methods of choice. Thus, the kinetic constants of peptide $Neu_{546-556}$ (DNLY-pYWDQNSS) for the *Yersinia* PTPase was determined by the inorganic phosphate colorimetric procedure (Table 2).

Initial Rate Analysis

In order to validate the progress curve analysis, we also conducted initial rate analysis on some of the peptide substrates using the inorganic phosphate assay procedure. Figure 4 shows a typical v vs [s] Michaelis–Menten hyperbolic curve for the Yop51* catalyzed hydrolysis of $Neu_{347-357}$ at pH 6.6, 30°C. A k_{cat} of 1306 ± 50 s^{-1} and a K_m of 74.5 ± 6.5 μM were determined from a direct fit of the v vs [s] data to the Michaelis–Menten equation using the nonlinear regression program Enzfitter (24), with excellent agreement between the two assays.

DISCUSSION

The analysis of the progress curves of enzyme-catalyzed reactions has often been regarded as being an attractive alternative to initial-rate methods for the determination of kinetic parameters (25). The attraction of

TABLE 1

Difference Molar Absorption Coefficients of Tyrosine-Phosphorylated and -Dephosphorylated Peptide

pH	4.6	5.0	5.5	6.0	6.6	7.0	7.6	8.0	8.4	9.0
$\Delta\epsilon_{282}$	968	999	998	931	874	826	834	865	858	891

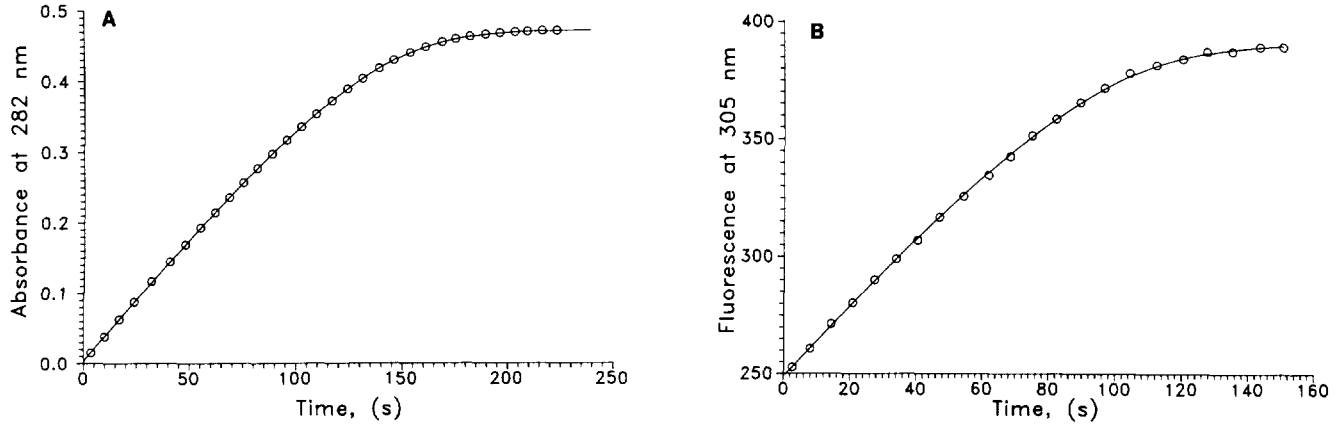

FIG. 2. Progress curve analysis of PTPase-catalyzed hydrolysis of phosphotyrosine-containing peptide. (A) A typical time course of the increase in absorbance at 282 nm during the Yop51*-catalyzed hydrolysis of $p60^{src}$ at pH 6.6, 50 mM 3,3-dimethylglutarate, 1 mM EDTA, I = 0.15 M buffer, and 30°C. The peptide substrate concentration was 500 μM and the enzyme concentration was 3.45 nM. (B) A typical time course of the increase in fluorescence at 305 nm during the PTP1U323-catalyzed hydrolysis of $Neu_{347-357}$ at pH 6.6, 50 mM 3,3-dimethylglutarate, 1 mM EDTA, I = 0.15 M buffer, and 30°C. The peptide substrate concentration was 15 μM and the enzyme concentration was 2.67 nM. The theoretical curve (solid line) was obtained through a nonlinear least squares fit algorithm to the experimental data (O) using the integral Michaelis–Menten equation.

this approach lies in the use of the entire progress curve in the analysis of the kinetic parameters rather than just a small part of it. The initial rate and the final stage of a reaction are the most difficult portions to measure accurately (25). The advance in computer technology for data acquisition on instruments used to measure enzyme kinetics has made it feasible and desirable to use complete progress curves for such analyses. One of the approaches used in the analysis of progress course is the integral method, in which data in the form of time vs [product] or [substrate] are fitted to the integral rate equation. There are two advantages of such an approach: (i) the need to differentiate the data (i.e., measure rates) is eliminated; (ii) more of the available information is utilized and thus the number of experiments to be performed is reduced, with a resultant saving of time and materials (26). Given a large number of evenly distributed experimental data pairs and a truly random error associated with the p values, the nonlinear least squares regression analysis will yield optimized parameters which differ from their true values by less than the standard deviation associated with these parameters. A side benefit of this method is that it is not necessary to convert the experimental variables (e.g., absorbance or fluorescence) into concentrations, since the conversion factors, the background to be subtracted, and the experimental variable at t = infinity can all be determined from the nonlinear least squares analysis as independent parameters. The analysis of the time course using the integrated equation give kinetic parameter which are comparable to the initial rate assay (see result), with a precision in most cases <10%.

The most severe practical limitation of any progress curve analysis occurs when the enzyme, substrates, or products show a significant degree of instability under the chosen assay conditions (21), so that the apparent decrease in velocity is not merely due to the depletion of substrate. In our case however, the products of PTPase-catalyzed hydrolysis of phosphotyrosine-containing peptides, (namely, inorganic phosphate and the dephos-

TABLE 2

Kinetic Constants for the Hydrolysis of Phosphorylated Peptides by Yersinia Protein Tyrosine Phosphatase at pH 6.6, 30°C

Substrate		K_m (μM)	k_{cat} (s^{-1})	$10^{-7} \times k_{cat}/K_m$ ($M^{-1}\ s^{-1}$)
DAEEpYLVPQQG	$Neu_{347-357}$	78.4 ± 1.6	1348 ± 8.3	1.72
DNLYpYWDQNSS	$Neu_{546-556}$	103 ± 28	446 ± 42	0.433
ENPEpYLGLDVPV	$Neu_{572-583}$	392 ± 20	1414 ± 41	0.361
EDNEpYTARE	$p56^{lck}_{390-398}$	2240 ± 45	1676 ± 24	0.0748
TEPQpYQPGE	$p60^{src}_{523-531}$	390 ± 6.0	1287 ± 9	0.330
AcRRLIEDAEpYAARG	(RR-src)	189 ± 24	1178 ± 100	0.623

TABLE 3

Kinetic Constants for the Hydrolysis of Phosphorylated Peptides by Rat PTP1U323 at pH 6.6, 30°C

Substrate		K_m (μM)	k_{cat} (s^{-1})	$10^{-7} \times k_{cat}/K_m$ ($M^{-1}\ s^{-1}$)
DAEEpYLVPQQG	$Neu_{347-357}$	3.52 ± 0.72	71.0 ± 2.3	2.02
DNLYpYWDQNSS	$Neu_{546-556}$	3.40 ± 0.59	55.7 ± 0.92	1.64
ENPEpYLGLDVPV	$Neu_{572-583}$	6.77 ± 0.79	85.6 ± 0.96	1.26
EDNEpYTARE	$p56^{lck}_{390-398}$	10.1 ± 1.6	74.8 ± 1.0	0.740
TEPQpYQPGE	$p60^{src}_{523-531}$	6.16 ± 0.20	78.9 ± 0.17	1.28
AcRRLIEDAEpYAARG	(RR-src)	8.60 ± 0.49	55.9 ± 0.38	0.65

phorylated peptide) are very stable. Nonenzymatic hydrolysis of the substrates, i.e., the phosphotyrosine-containing peptides, was undetectable under the assay conditions. Furthermore, both Yop51* and PTP1U323 were stable under the assay conditions employed here.

One other cautionary note is the possible existence of product inhibition. Inorganic phosphate is a competitive inhibitor for both Yop51* and PTP1U323 with K_i values of 5.5 and 3.4 mM at pH 6.6 and 30°C, respectively. Under the assay conditions used here the substrate concentrations were much below 1 mM, and the production of inorganic phosphate did not show any noticeable effects on the progress curve. This was confirmed by the fact that progress curve analysis at two different substrate concentrations gave identical results. This was also supported by independent initial rate analyses which yielded identical kinetic parameters when compared to the progress curve analysis under identical conditions. In addition, the other product, the dephosphorylated peptide, did not show any inhibition at concentrations in the range of 0.6–1 mM. Similar observations have been made for the LAR-D1-catalyzed hydrolysis of peptide substrates (9). These observations demonstrate that the phosphotyrosyl residue is crucial for phosphatase substrate recognition. Even for cases where there is significant product inhibition, appropriate rate equations have been derived which incorporate the inhibition constants to allow adequate analysis of the time course using the integrated equations (21,22). One can also easily adopt the described spectrophotometric and fluorimetric properties for initial rate assays where the problem of product inhibition is minimized.

There are two practical limitations pertinent to the method described in this paper. The present assay is not suitable for substrates with multiple tyrosine phosphor-

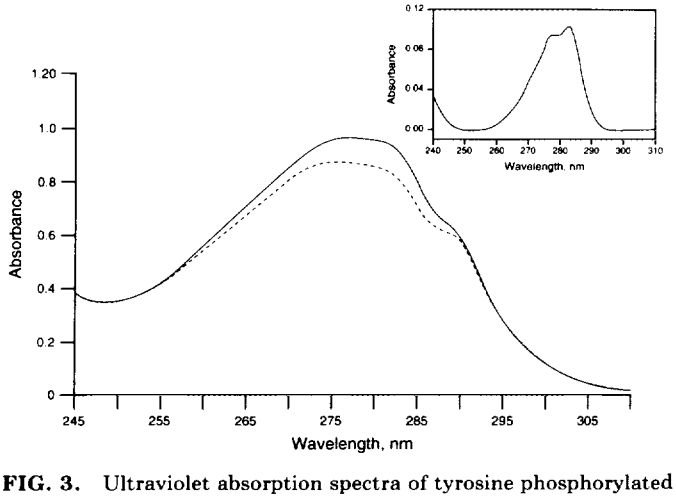

FIG. 3. Ultraviolet absorption spectra of tyrosine phosphorylated $Neu_{546-556}$. Spectra were taken at 25°C, in 50 mM 3,3-dimethylglutarate, 1 mM EDTA, I = 0.15 M, pH 6.6, buffer. The peptide $Neu_{546-556}$ concentration was 104 μM. Solid line, dephosphorylated peptide $Neu_{546-556}$; dashed line, tyrosine phosphorylated peptide $Neu_{546-556}$. Inset, the difference spectrum of the tyrosine-dephosphorylated and -phosphorylated $Neu_{546-556}$.

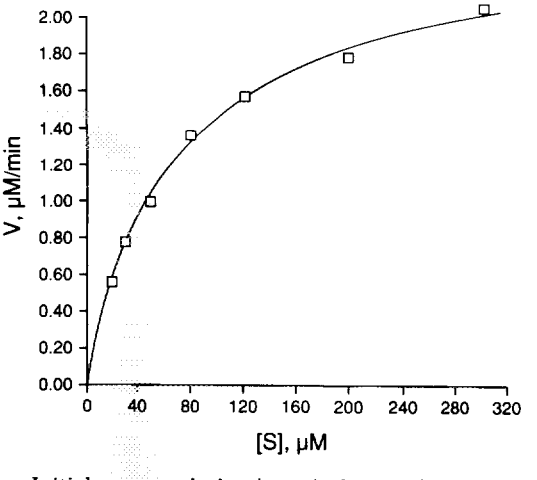

FIG. 4. Initial rate analysis. A typical v vs [s] curve for the Yop51*-catalyzed hydrolysis of $Neu_{347-357}$ using inorganic phosphate assay procedure. Reactions were conducted as described under Methods and data were obtained under conditions where <10% of the substrates was converted to products to ensure initial rate requirements. The theoretical curve (solid line) was generated by the Enzfitter program (21) to the experimental data (□) using the Michaelis–Menten equation.

ylations, since only the gross change in absorbance or fluorescence will be followed. However, HPLC (27) and NMR (28) techniques have recently been applied to these systems to monitor the dephosphorylation of individual tyrosine residues. Another potential problem results from the fact that measurements are conducted at a wavelength where proteins absorb and fluorescence. Therefore, the present assay is not ideal for monitoring low PTPase activity in crude extracts which give high background signals. The assay is still applicable when there is only moderate background absorbance, as was demonstrated in the result for peptide $Neu_{546-556}$ (DNLYpYWDQNSS) which has additional Trp and Tyr residues in the peptide.

The absorption and fluorescence techniques described above are complementary. The lower detection limit of the inorganic phosphate colorimetric determination is in the nmols range (29,30). Under initial rate conditions where less than 5% of substrate is consumed, the lowest amount of substrate one should use is 20 nmol, which translates into 40 μM in 0.5 ml reaction mixture. Therefore, only K_m values in the magnitude of at least 100 μM can be reliably determined using the inorganic phosphate assay procedure. In our continuous spectrophotometric assay, peptide substrates with K_m values from μM to mM can be routinely determined, so that the present spectrophotometric assay is not only more convenient but also as sensitive as the widely used inorganic phosphate assay. In cases where the K_m value is below 1 μM, the fluorescence technique is more appropriate. Under these conditions the "inner filter" effect due to the inherent absorption of the peptides is insignificant, and fluorescence techniques are usually much more sensitive than absorption.

As has been suggested by Zhao *et al.* (12), one can theoretically take advantage of the described properties of tyrosine absorbance and fluorescence upon phosphorylation to follow the protein tyrosine kinase-catalyzed phosphorylation reaction where the decrease in absorbance or fluorescence on tyrosine residue is monitored. The methodology described here could be easily adapted in this regard. Although the physiological substrates of tyrosine kinases and PTPases await identification, *in vitro* studies employing artificial substrates and synthetic peptides have proven useful in the characterization of protein kinases. It has been shown from model peptide studies that the amino acid sequence of the substrate plays a crucial role in selection of phosphorylation sites for protein kinases and "consensus sequences" have been elucidated for different classes of protein kinases (31). Yop51* shows substantial discrimination in molecular recognition of phosphotyrosyl containing peptides even in the context of nona- to dodecapeptides. The reason that PTP1U323 does not display much selectivity against the same set of peptides is unclear. However the mammalian phosphatase is localized on the ER (32,33), and the intracellular localization of the PTPase may play an important role in dictating its specificity. While much progress has been made in the identification and characterization of PTPases, limited information is available about their mechanism of action or substrate specificity. A complete understanding of the kinetic and chemical mechanisms of PTPase-catalyzed dephosphorylation reactions and the requirements of a consensus peptide sequence for substrate recognition will be invaluable. The continuous assay systems described in this paper should facilitate such investigations.

ACKNOWLEDGMENTS

We are grateful for the constructive comments of Dr. Ferenc J. Kézdy (Biochemistry Unit, The Upjohn Co.). We thank Dr. Alan Saltiel and Dr. Tomi Sawyer (Parke-Davis Research Division, Warner Lambert Co.) for their support. This work was supported by a grant from the National Institutes of Health, NIDDKD 18849, and the Walther Cancer Institute.

REFERENCES

1. Yarden, Y., and Ullrich, A. (1988) *Annu. Rev. Biochem.* **57,** 443–478.
2. Fischer, E. H., Charbonneau, H., and Tonks, N. K. (1991) *Science* **253,** 401–406.
3. Tonks, N. K., Diltz, C. D., and Fischer, E. H. (1988) *J. Biol. Chem.* **263,** 6731–6737.
4. Tonks, N. K., Diltz, C. D., and Fischer, E. H. (1990) *J. Biol. Chem.* **265,** 10674–10680.
5. Guan, K. L., and Dixon, J. E. (1990) *Science* **249,** 553–556.
6. Pallen, C. J., Lai, D. S. Y., Chia, H. P., Boulet, I., and Tong, P. H. (1991) *Bichem. J.* **276,** 315–323.
7. Hudson, D. (1988) *J. Org. Chem.* **53,** 617–624.
8. Kitas, E. A., Perich, J. W., Wade, J. D., John, R. B., and Tregear, G. W. (1989) *Tetrahedron Lett.* **30,** 6229–6232.
9. Cho, H., Ramer, S. E., Itoh, M., Winkler, D. G., Kitas, E., Bannwarth, W., Burn, P., Saito, H., and Walsh, C. T. (1991) *Biochemistry* **30,** 6210–6216.
10. Madden, J. A., Bird, M. I., Man, Y., Raven, T., and Myles, D. D. (1991) *Anal. Biochem.* **199,** 210–215.
11. Apostol, I., Kuciel, R., Wasylewska, E., and Ostrowski, W. S. (1985) *Acta Biochim. Polonica* **32,** 187–197.
12. Zhao, Z., Zander, N. F., Malencik, D. A., Anderson, S. R., and Fischer, E. H. (1992) *Anal. Biochem.* **202,** 361–366.
13. Zhang, Z.-Y., Clemens, J. C., Schubert, H. L., Stuckey, J. A., Fischer, M. W. F., Hume, D. M., Saper, M. A., and Dixon, J. E. (1992) *J. Biol. Chem.* **267,** 23759–23766.
14. Guan, K. L., and Dixon, J. E. (1991) *Anal. Biochem.* **192,** 262–267.
15. Steward, J. M., and Young, J. D. (1984) Solid Phase Peptide Synthesis, 2nd ed., Pierce Chemical Co., Rockford, IL.
16. Perich, J. W., and Johns, R. B. (1988) Synthesis, pp. 142–144.
17. Tian, Z., Gu, C., Roeske, R. W., Zhou, M., and Van Etten, R. L. (1993) *Int. J. Peptide Protein Res.*, in press.

18. Pike, L. J., Eakes, A. T., and Krebs, E. G. (1986) *J. Biol. Chem.* **261,** 3782–3789.
19. Zhang, Z.-Y., and Van Etten, R. L. (1991) *J. Biol. Chem.* **266,** 1516–1525.
20. Segel, I. H. (1975) *in* Enzyme Kinetics, p. 54, Wiley, New York.
21. Duggleby, R. G., and Morrison, J. F. (1977) *Biochim. Biophys. Acta* **481,** 297–312.
22. Koerber, S. C., and Fink, A. L. (1987) *Anal. Biochem.* **165,** 75–87.
23. Yamaoka, K., Tanigawara, Y., Nakagawa, T., and Uno, T. (1981) *J. Pharmacobio-Dyn.* **4,** 879–885.
24. Leatherbarrow, R. J. (1987) Enzfitter: A Non-linear Regression Data Analysis Program for the IBM PC, Elsevier Science, Amsterdam.
25. Orsi, B. A., and Tipton, K. F. (1979) *Methods Enzymol.* **63,** 159–183.
26. Cornish-Bowden, A. J. (1972) *Biochem. J.* **130,** 637–639.
27. Ramachandran, C., Aebersold, R., Tonks, N. K., and Pot, D. A. (1992) *Biochemistry* **31,** 4232–4238.
28. Lee, J. P., Cho, H., Bannwarth, W., Kitas, E. A., and Walsh, C. T. (1992) *Protein Science* **1,** 1352–1362.
29. Lanzetta, P. A., Alvarez, L. J., Reinach, P. S., and Candia, O. A. (1979) *Anal. Biochem.* **100,** 95–97.
30. Black, M. J., and Jones, M. E. (1983) *Anal. Biochem.* **135,** 233–238.
31. Kennelly, P. J., and Krebs, E. G. (1991) *J. Biol. Chem.* **266,** 15555–15558.
32. Frangioni, J. V., Beahm, P. H., Shifrin, V., Jost, C. A., and Neel, B. G. (1992) *Cell* **68,** 545–560.
33. Woodford-Thomas, T. A., Rhodes, J. D., and Dixon, J. E. (1992) *J. Cell Biol.* **117,** 401–404.